

Evaluating a high-resolution urban fossil CO₂ emissions inventory using eddy-covariance flux measurements and source partitioning

Kai Wu^{1,*}, Kenneth J. Davis^{1,2}, Natasha L. Miles¹, Scott J. Richardson¹,
Thomas Lauvaux³, Daniel P. Sarmiento⁴, Nikolay V. Balashov⁴, Klaus
Keller^{5,2}, Jocelyn Turnbull^{6,7}, Kevin R. Gurney^{8,9}, Jianming Liang⁹, Geoffrey
Roest⁸

¹Department of Meteorology and Atmospheric Science, The Pennsylvania State University, University
Park, Pennsylvania 16802, United States

²Earth and Environmental Systems Institute, The Pennsylvania State University, University Park,
Pennsylvania 16802, United States

³Laboratoire des Sciences du Climat et de l'Environnement, CEA, CNRS, UVSQ/IPSL, Université
Paris-Saclay, Orme des Merisiers, 91191 Gif-sur-Yvette Cedex, France

⁴NASA Goddard Space Flight Center, Greenbelt, Maryland 20771, United States

⁵Department of Geosciences, The Pennsylvania State University, University Park, Pennsylvania 16802,
United States

⁶Rafter Radiocarbon Laboratory, GNS Science, Lower Hutt 5040, New Zealand

⁷CIRES, University of Colorado at Boulder, Boulder, Colorado 80309, United States

⁸School of Informatics, Computing and Cyber Systems, Northern Arizona University, Flagstaff, Arizona
85287, United States

⁹School of Life Sciences, Arizona State University, Tempe, Arizona 85281, United States

*now at: School of GeoSciences, The University of Edinburgh, Edinburgh, United Kingdom

Key Points:

- Urban CO₂ flux measurements are partitioned into fossil and biogenic components using CO and ¹⁴C measurements and a flux-gradient method.
- The partitioned fossil CO₂ emissions show remarkable consistency of the comparison with an emissions inventory in time and space.
- Biogenic CO₂ fluxes within the city are non-negligible in the cold season and need to be considered in urban CO₂ monitoring.

Corresponding author: Kai Wu, kwu2@ed.ac.uk

Abstract

We present the first quantitative comparison of source-partitioned CO₂ flux measurements with a high-resolution urban fossil CO₂ emissions inventory. We use tower-based measurements of CO and ¹⁴C to partition net CO₂ flux measurements into fossil and biogenic components in a suburban environment. A flux footprint model is used to quantify spatial patterns in fluxes. The partitioned fossil CO₂ emissions are compared to a 200-m resolution emissions inventory (Hestia). The results indicate that Hestia and the partitioned flux data agree remarkably well on a seasonal average scale. The Hestia inventory is biased by 3.2% (cold season) and 9.1% (warm season). Their temporal-spatial patterns match closely. In addition, biogenic CO₂ uptake is 25% of local fossil emissions during afternoon in the cold season. This work demonstrates the effectiveness of using eddy-covariance flux measurements both for evaluating urban emissions inventories and for quantifying urban ecosystem fluxes.

Plain Language Summary

This work presents the first comparison of two innovative approaches for quantifying urban CO₂ emissions from the combustion of fossil fuels. Both approaches can quantify emissions from neighborhoods with hourly time resolution. These methods show very similar results concerning the seasonal-mean fossil CO₂ emissions, as well as the emissions variation in time and space. We also find relatively large biological CO₂ exchange, even during winter when the biosphere is often assumed to be dormant. The results show great promise for these new methods of quantifying source, space and time resolved CO₂ exchanges, and emphasize the need to take biological CO₂ fluxes into account when attempting to quantify fossil CO₂ emissions using atmospheric measurements.

1 Introduction

Cities are becoming the focus for formulating and implementing carbon dioxide (CO₂) emissions mitigation efforts (Hutyra et al., 2014; Lee & Koski, 2014; Bulkeley, 2013). Evaluating the effectiveness of emissions reduction efforts requires accurate and independent CO₂ emissions estimates (Lauvaux et al., 2020; Turnbull et al., 2018). Although cities cover only 3% of the global land area, urban areas are home to 55% of the world's population, a proportion that is expected to increase to 68% by 2050 (Chaouad & Verzeoli, 2018). Overall, more than 70% of global fossil fuel CO₂ (CO₂ff) emissions are from urban areas (Edenhofer et al., 2015). Efforts to assess and mitigate CO₂ emissions can provide benefits for urban sustainability and balanced economic growth (Hsu et al., 2019).

Urban areas are consistently reported as a net source of CO₂ (Velasco & Roth, 2010). The temporal variation of urban CO₂ is dependent on human activities and urban ecosystems (McKain et al., 2012; Pataki et al., 2006). The eddy-covariance technique has been applied to measure urban CO₂ emissions for about two decades. This method has been demonstrated in many cities (Björkegren & Grimmond, 2018; Ao et al., 2016; Lietzke et al., 2015; Järvi et al., 2012; Christen et al., 2011; Vogt et al., 2006; Nemitz et al., 2002; Grimmond et al., 2002). The attribution of urban CO₂ flux measurements is challenging due to the spatial heterogeneity, mixed emission sources and sinks, and limited spatial coverage of flux measurements (Aubinet et al., 2012). Although most of urban flux studies focus on the total observed CO₂ flux, a few studies attempt to partition net flux measurements into fossil and biogenic components accounting for the temporal and spatial variability of the multiple sources and sinks. Menzer and McFadden (2017) modeled fossil CO₂ emissions based on winter data and extrapolated them to the growing season to estimate biogenic fluxes. Ishidoya et al. (2020) demonstrated partitioning of CO₂ fluxes into liquid and gaseous fossil fuel components using O₂ and CO₂ measurements.

78 Sugawara et al. (2021) used a nearby tower to estimate the biogenic component of a total
79 CO₂ flux measurement.

80 Quantification of anthropogenic CO₂ emissions is challenging due to the difficulty
81 of separating CO₂ff emissions from biogenic CO₂ (CO₂bio) fluxes (Miller et al., 2020;
82 Basu et al., 2020; Menzer & McFadden, 2017; Pataki et al., 2007). Previous studies have
83 demonstrated the feasibility of using ¹⁴C isotope measurements to separate CO₂ff from
84 CO₂bio fluxes (Basu et al., 2016; Turnbull et al., 2015; Miller et al., 2012), but flask mea-
85 surements of ¹⁴C are expensive and discontinuous. Continuous measurements of carbon
86 monoxide (CO) provide another approach to track CO₂ff emissions (Silva et al., 2013;
87 Levin & Karstens, 2007; Turnbull et al., 2006). Uncertainties in the CO to CO₂ff ratio,
88 which vary as a function of emission sectors, complicate the attribution of urban CO₂
89 fluxes. These methods have not yet been applied to eddy-covariance flux measurements.

90 Emissions inventories use activity data to aggregate source-specific and total emis-
91 sions (Boden et al., 2009; Gurney et al., 2009; Olivier & Janssens-Maenhout, 2012), but
92 the differences among inventories are sizeable (Gately & Hutyra, 2017; Oda et al., 2019).
93 Atmospheric inversions use inventories as prior estimates of emissions and optimize the
94 emissions using atmospheric mole fraction observations (Bréon et al., 2015; Turner et al.,
95 2016; Stauder et al., 2016; Lauvaux et al., 2016; Kunik et al., 2019; Lauvaux et al., 2020).
96 Determination of the uncertainty in the inversion results hinges on estimates of errors
97 in atmospheric transport models (Deng et al., 2017; Sarmiento et al., 2017) and emis-
98 sions inventories (Wu et al., 2018). The Hestia emissions inventory (Gurney et al., 2012)
99 was developed in part to support the Indianapolis Flux Experiment (INFLUX) and uses
100 energy consumption, population density, and traffic data to quantify CO₂ff emissions for
101 an entire urban landscape at an approximately 200-m and hourly resolution. The high-
102 resolution performance of the Hestia inventory has not yet been evaluated using atmo-
103 spheric observations.

104 This study compares seven months of source-partitioned CO₂ eddy-covariance flux
105 measurements with a high-resolution emissions inventory (Hestia) in a suburban region
106 of Indianapolis, Indiana, USA. We partition the total CO₂ flux measurements into CO₂ff
107 and CO₂bio components using a flux-gradient relationship (Stull, 2012; Ishidoya et al.,
108 2020) and atmospheric CO measurements. ¹⁴C isotope measurements are used to esti-
109 mate the CO to CO₂ff ratio and reduce the uncertainty in the flux decomposition. Our
110 source decomposition methods are similar to those used by Ishidoya et al. (2020) and
111 Sugawara et al. (2021). In addition, we use a flux footprint model (Kljun et al., 2015,
112 2004) to match each flux measurement in space and time with the Hestia inventory to
113 provide a direct comparison of independent estimates of fossil CO₂ emissions at high spa-
114 tial and temporal resolution. This is, to our knowledge, the first such comparison of these
115 innovative and independent assessments of high-resolution urban CO₂ emissions, and is
116 timely given the growing interest in studies of urban systems.

117 2 Data and Methods

118 2.1 Site Descriptions and Atmospheric CO₂ Flux Measurements

119 The INFLUX observation network (Davis et al., 2017) measures atmospheric CO₂
120 and CO mole fractions, and net CO₂ fluxes in and around Indianapolis, IN (Figure 1).
121 The locations, sampling heights and measurements at these sites are described by Miles
122 et al. (2017) and instrument performance by Richardson et al. (2017). ¹⁴C isotope mea-
123 surements, which are related to CO₂ff emissions, are collected weekly using a flask sam-
124 pling system (Turnbull et al., 2015). We focus on seven months (January to July, 2013)
125 of eddy-covariance flux measurements at Tower 2 located in a heterogeneous suburban
126 environment (Figures 1 and S1). There is a highway to the north, urban vegetation to
127 the south, and neighborhoods with detached houses. The heterogeneous surroundings

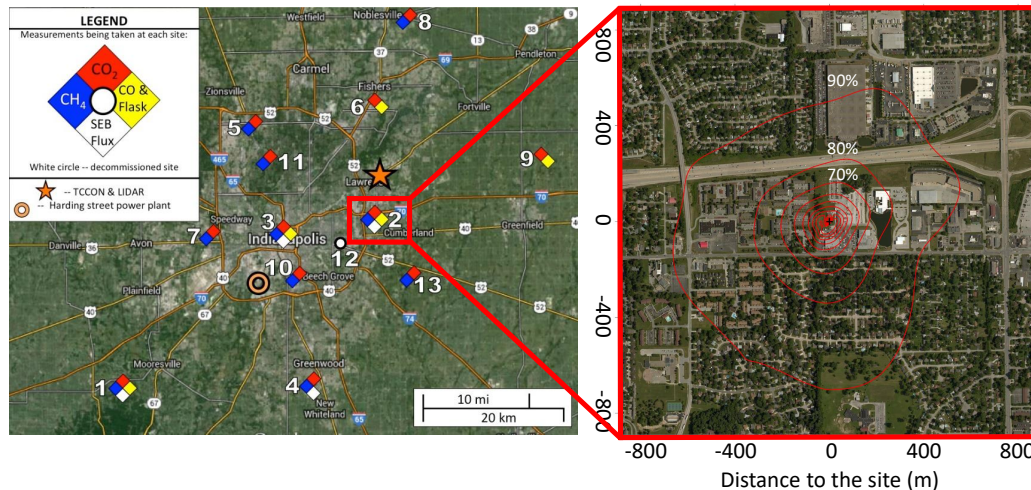


Figure 1. The Indianapolis Flux Experiment (INFLUX) measurement network in Indianapolis, IN (left) and cumulative flux footprints from January to July in 2013 at Tower 2 (right). The contours in the right panel represent the percentage of the time-integrated flux that comes from within that boundary. The color of the marker in the left panel represents the measurements at each site: red for CO₂, yellow for CO and ¹⁴C, blue for CH₄, and white for surface energy balance fluxes. The coordinates in the right panel are the distance (m) to the measurement site.

128 present a good test of our ability to partition net CO₂ flux measurements into biogenic
 129 and fossil fuel components.

130 The flux instrumentation, which includes a sonic anemometer (Campbell Scientific,
 131 CSAT-3) and a high-frequency open-path infrared CO₂ sensor (LI-COR Environmen-
 132 tal, LI-7500), is mounted at 30 m above ground level (AGL) on Tower 2. The eddy-covariance
 133 technique measures the covariance between fluctuations in vertical wind velocity and CO₂
 134 density to detect the integrated exchange of CO₂ between land and atmosphere (Lee et
 135 al., 2004; Foken & Napo, 2008; Aubinet et al., 2012). We use flux calculation and filter-
 136 ing methods recommended by Vickers and Mahrt (1997). We filter out extreme values
 137 outside 3.5 σ range of the data (0.2% of data are filtered out) and nighttime fluxes dur-
 138 ing weak turbulence conditions when the friction velocity is less than 0.2 m/s (3.6% of
 139 data are filtered out) (Gu et al., 2005). Negative fluxes confirm the predominant role of
 140 photosynthesis from the urban vegetation around this site (Figure S2). We define the
 141 cold season as January to March (JFM) and the warm season as April to July (AMJJ)
 142 based on the presence of negative total CO₂ fluxes during the daytime in the warm sea-
 143 son (Figure S3).

144 2.2 Partitioning Fossil Fuel and Biogenic CO₂ Fluxes

145 To partition fossil fuel and biogenic components from the net CO₂ flux measure-
 146 ments, we apply a flux-gradient method and atmospheric CO measurements. We mea-
 147 sure CO₂ and CO mole fractions at 10 m and 40 m heights AGL at Tower 2 (Miles et
 148 al., 2017). We use the eddy-covariance flux measurement and measured vertical gradi-
 149 ent in CO₂ to solve for the eddy diffusivity, and use that eddy diffusivity and the CO
 150 vertical gradient to solve for the CO flux, as shown in the supporting information. There
 151 are three assumptions in this method: (1) Turbulent eddies are small enough that lo-
 152 cal scalar gradients are proportional to turbulent fluxes; (2) CO and CO₂ are subject
 153 to the same vertical mixing processes; (3) Within the turbulent flux footprint, CO is mainly

154 produced by fossil fuel combustion. We filter out counter-gradient fluxes, and limit the
 155 eddy diffusivity and CO flux within 3.5σ range of their estimates to screen out extreme
 156 values caused by tiny denominators.

157 The emission ratio of CO to CO_{2ff} is estimated from flask measurements of ¹⁴C
 158 and CO measurements (Turnbull et al., 2015). The urban CO enhancements are esti-
 159 mated by the differences between Tower 2 and upwind background sites (Tower 1 or 9
 160 depending on the wind direction). The median and mean values of CO to CO_{2ff} ratios
 161 are 9.52 and 8.98 ppb ppm⁻¹ (cold season) and 9.13 and 9.02 ppb ppm⁻¹ (warm sea-
 162 son) (Figure S4). We use 9 ppb ppm⁻¹ as an approximate value to infer CO_{2ff} emissions.
 163 To test the uncertainty of using different ratios on the flux decomposition, we vary the
 164 emission ratio to 11 and 7 ppb ppm⁻¹ based on the range of values estimated by Turnbull
 165 et al. (2015). Since traffic emissions are likely to have a higher ratio and residential emis-
 166 sions have a smaller ratio. We add another scenario with a CO to CO_{2ff} ratio of 15 ppb
 167 ppm⁻¹ for northerly winds from the highway, and 7 ppb ppm⁻¹ for the other wind di-
 168 rections.

169 2.3 Flux Footprint and Emissions Inventory

170 A flux footprint, which is defined as the contributing area upwind from the mea-
 171 surement site (Leclerc & Foken, 2014), is essential to account for the spatial heterogene-
 172 ity of emission sources. We use a two-dimensional flux footprint model (Kljun et al., 2015,
 173 2004) to match with the Hestia inventory. Tower-based measurements of wind field and
 174 boundary layer characteristics are used to estimate the input parameters of the footprint
 175 model (*i.e.* roughness length, Obukhov length, friction velocity, standard deviation of
 176 lateral velocity fluctuations, etc.). The size of footprint depends on measurement height,
 177 surface roughness, and atmospheric thermal stability. The footprint will increase with
 178 an increase in measurement height, with a decrease in surface roughness, and with an
 179 increase in atmospheric thermal stability (Burba & Anderson, 2010). The spatial res-
 180 olution of the footprint model is approximately two meters. We match every flux foot-
 181 print with Hestia via a convolution of the influence function with the Hestia emissions.

182 3 Results

183 Net CO₂ flux measurements, decomposed as a function of time and space, behave
 184 as expected given the environment surrounding the tower. Observed CO₂ emissions are
 185 larger in the cold season than the warm season (Figure 2a), perhaps due to increased emis-
 186 sions from building heating around the tower (Figures 1 and S1). In the cold season, there
 187 are two prominent peaks in emissions likely corresponding to peaks in traffic volume dur-
 188 ing rush hours. In the warm season, fossil fuel CO₂ emissions are mixed with photosyn-
 189 thesis and respiration from urban vegetation within the flux footprints. The daytime pho-
 190 tosynthetic uptake of CO₂ indicates the role of urban vegetation. The spatial patterns
 191 of flux data show high emissions from the north, and lower emissions or net uptake from
 192 the south (Figures 2b and 2c), consistent with the highway to the north and urban veg-
 193 etation to the south of the tower (Figures 1 and S1).

194 Partitioning of the net observed CO₂ fluxes into fossil and biogenic components yields
 195 broadly plausible temporal behavior of these flux components (Figure 3). While substan-
 196 tially smaller than the estimated CO_{2ff} emissions, the cold season CO_{2bio} uptake is 25%
 197 of urban CO_{2ff} emissions during the afternoon (Figure 3a), which is non-negligible and
 198 need to be considered to obtain accurate CO_{2ff} emissions. A typical pattern of ecosys-
 199 tem fluxes emerges in the warm season (Figure 3b). The warm season CO_{2bio} fluxes are
 200 equal in amplitude to the CO_{2ff} emissions, emphasizing the importance of accounting
 201 for CO_{2bio} fluxes in attempts to quantify urban CO_{2ff} emissions.

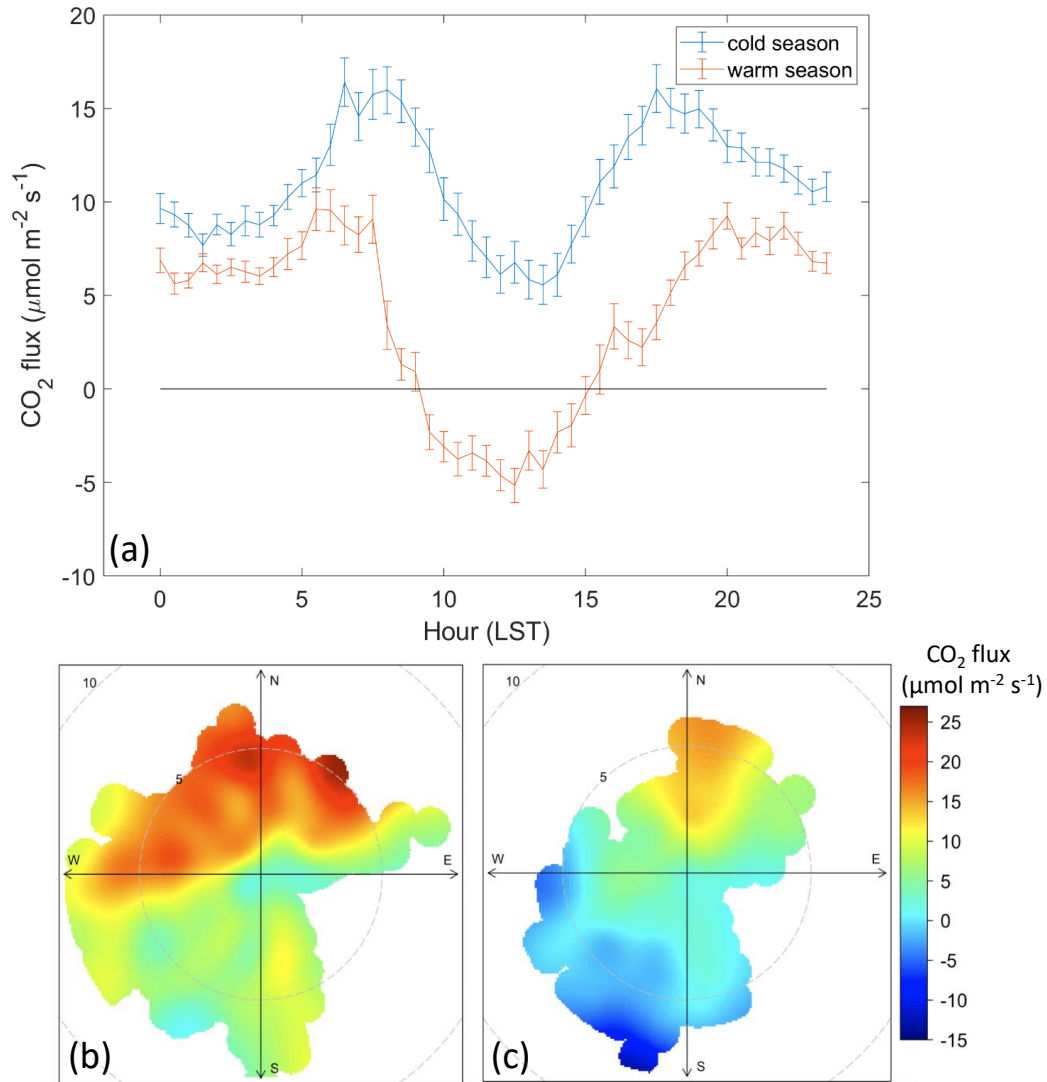


Figure 2. Diurnal variation of seasonally-averaged CO₂ flux measurements during the cold (JFM) and warm (AMJJ) seasons in 2013 (a). Error bars indicate the standard errors of the seasonal means. Spatial variation of time-averaged CO₂ fluxes in the cold (b) and warm (c) seasons. Color indicates flux magnitude. The radial coordinate corresponds to wind speed (m s^{-1}) and the polar coordinate defines wind direction.

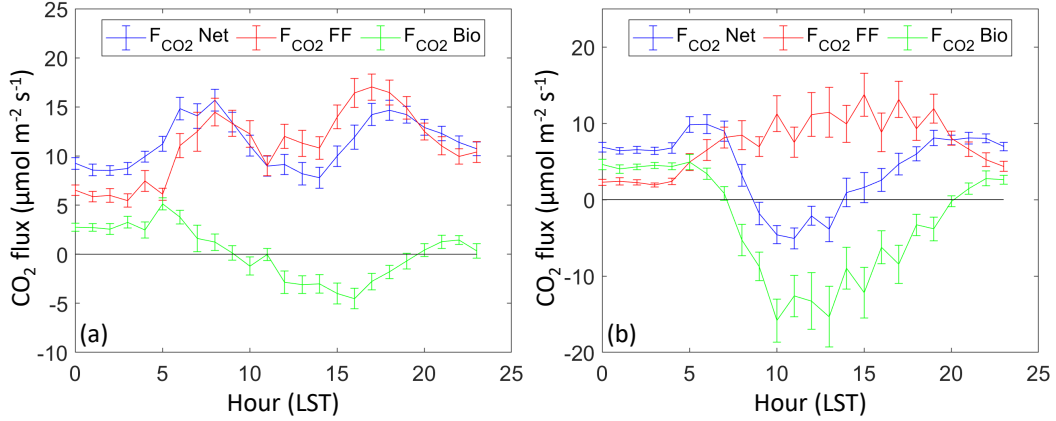


Figure 3. Diurnal variation of seasonally-averaged net CO₂ flux measurements (F_{CO_2Net}) and the partitioned fossil fuel (F_{CO_2FF}) and biogenic (F_{CO_2Bio}) fluxes in the cold (JFM) (a) and warm (AMJJ) (b) seasons in 2013. Error bars are the standard errors of the seasonal means.

202 The seasonally-averaged eddy-covariance CO_{2ff} emissions estimates show remark-
 203 able similarity to the Hestia inventory when matched in space and time using flux foot-
 204 prints. Seasonal-mean CO_{2ff} emissions differ (Hestia minus OBS) by $0.36 \mu\text{mol m}^{-2} \text{s}^{-1}$
 205 (3.2% of the mean partitioned CO_{2ff} emissions) in the cold season (Figure 4a) and 0.62
 206 $\mu\text{mol m}^{-2} \text{s}^{-1}$ (9.1% of the mean partitioned CO_{2ff} emissions) in the warm season (Fig-
 207 ure 4b). The corresponding root mean square errors (RMSEs) are $8.91 \mu\text{mol m}^{-2} \text{s}^{-1}$
 208 and $7.54 \mu\text{mol m}^{-2} \text{s}^{-1}$, which include random measurement errors in the flux data.

209 The temporal patterns of seasonally-averaged Hestia and eddy-covariance CO_{2ff}
 210 emissions also agree remarkably well (Figures 4c and 4d). The correlation coefficients
 211 of the seasonal-mean diurnal variations are 0.86 (cold season) and 0.93 (warm season).
 212 The Hestia emissions are smaller during the night and higher during the day compared
 213 to the partitioned observations in the cold season (Figures 4c and S5a), and consistently
 214 slightly higher than the partitioned observations in the warm season (Figures 4d and S5b).

215 We also find consistency in the comparison of eddy-covariance and Hestia CO_{2ff}
 216 emissions as a function of wind direction (Figure S6 and Table 1). In the cold season,
 217 the Hestia emissions are higher than the observed CO_{2ff} emissions for all wind directions
 218 except the north, west and northwest wind (Table 1). A similar pattern exists in the warm
 219 season. Since residential buildings lie upwind in the west and northwest wind directions
 220 (Figures 1 and S1), we infer that residential emissions may be the source of this discrep-
 221 ancy.

222 These results are somewhat sensitive to the choice of CO to CO_{2ff} emission ratio
 223 in the flux decomposition. Seasonal-mean flux bias and bias percentage change signif-
 224 icantly when the emission ratio varies from 9 ppb ppm⁻¹ to 11 or 7 ppb ppm⁻¹ (Table
 225 S1 and Figure S7a). The temporal variations are not highly sensitive to this choice (Fig-
 226 ure S7b). The scenario with the space-varying emission ratio (15 & 7 ppb ppm⁻¹), which
 227 may be more realistic than a constant ratio, does not significantly change compared to
 228 the default scenario (9 ppb ppm⁻¹) either the comparison of the diurnal variation (Fig-
 229 ure S7b) or the bias estimation (Table S1).

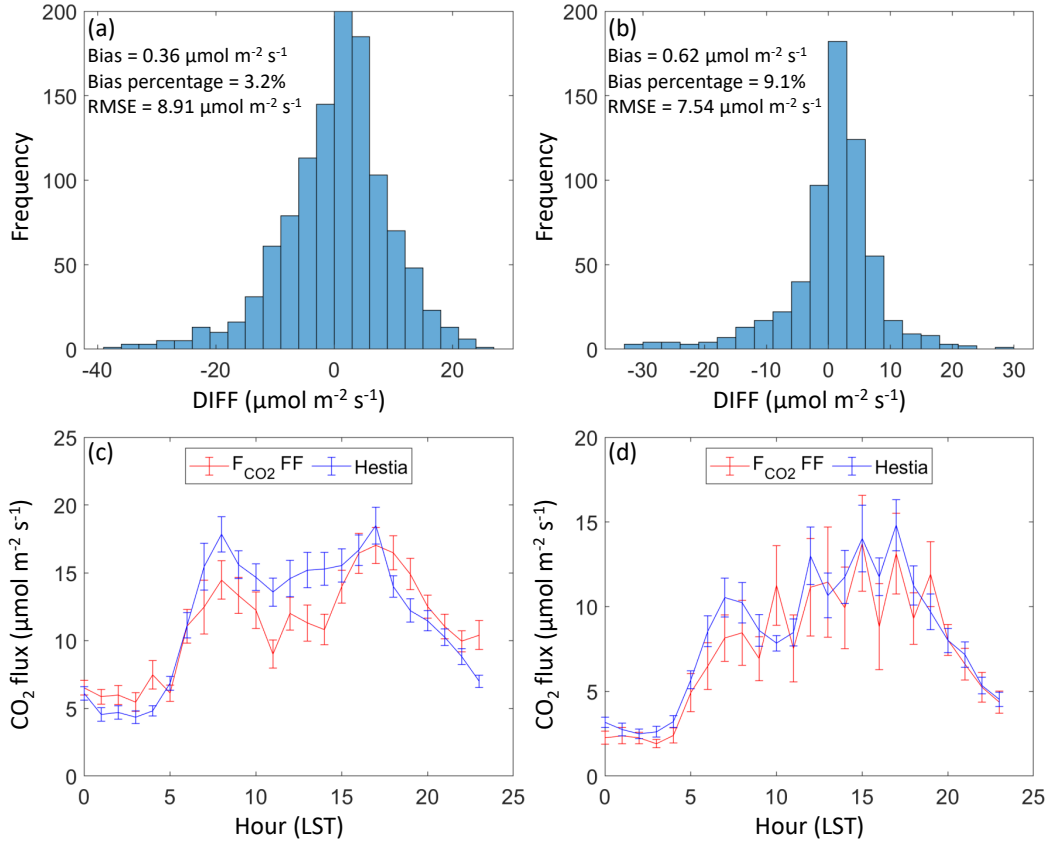


Figure 4. Histogram of flux differences between the Hestia inventory and the partitioned fossil fuel CO₂ emissions (Hestia minus OBS) in the cold (JFM) (a) and warm (AMJJ) (b) seasons in 2013. Bias, bias percentage compared to the mean partitioned CO₂ff emissions, and root mean square error (RMSE) are listed. Diurnal variation of seasonally-averaged CO₂ff emissions in the cold (c) and warm (d) seasons. Error bars are the standard errors of the seasonal means.

Table 1. Statistics of flux differences ($\mu\text{mol m}^{-2} \text{s}^{-1}$) between the Hestia inventory and the partitioned fossil fuel CO₂ emissions (Hestia minus OBS) for different wind directions.

	DIFF	N	NE	E	SE	S	SW	W	NW
Cold Season (JFM)	Median	-2.00	3.32	2.88	3.45	4.14	3.15	-4.47	-2.14
	Mean	-1.93	5.88	4.88	3.58	3.84	1.89	-4.72	-1.87
	RMSE ^a	10.98	9.27	8.22	5.63	7.45	8.00	10.40	9.06
Warm Season (AMJJ)	Median	2.49	3.34	1.92	1.98	0.98	0.42	-2.71	-4.27
	Mean	5.31	3.61	0.92	1.37	0.52	-1.32	-4.17	-5.21
	RMSE	8.24	9.32	5.19	5.54	5.97	8.62	8.47	13.66

^aroot mean square error

4 Conclusions and Discussion

The remarkably close agreement between the Hestia inventory and the partitioned eddy-covariance flux measurements suggests that both methods have the ability to quantify urban fossil CO₂ emissions. Neither approach has yet been cross-validated at such a high spatial and temporal resolution. The flux measurement partitioning is sensitive to the CO to CO₂ff emission ratio, but the consistency of Hestia and flux data suggests that flask measurements have accurately quantified that ratio. These results need to be tested at other locations and over different periods of time. The success of this test suggests that these eddy-covariance flux decomposition methods can be used to quantify source-specific CO₂ emissions of neighborhood-scale urban metabolic processes. Further the successful comparison to Hestia suggests that the algorithms and input data used in the inventory system are accurate and precise even down to the fine resolution of the eddy-covariance flux measurements.

This study also shows the promise of using this approach for studying urban ecosystem CO₂ fluxes. Previous work has suggested that the edges found in urban ecosystems lead to fundamentally different behavior of these ecosystems (Reinmann et al., 2020), but these findings are largely based on chamber-scale flux measurements. It is not clear whether or not, when upscaled to spatial domains that integrate across many edges such as a suburban forest, existing ecosystem models and model parameters will suffice in describing urban CO₂bio fluxes. Current ecosystem models used in urban studies are largely devoid of urban ecosystem flux measurements in either calibration or evaluation due to lack of data (Wu et al., 2021; Hardiman et al., 2017). We suggest that the decomposition methods can serve as a new approach for obtaining ecosystem flux data necessary to develop the next generation of urban ecosystem models.

Finally, this study emphasizes the importance of urban ecosystem fluxes, both in the growing/warm season and the dormant/cold season. The importance of these fluxes has been shown in multiple observational (Miller et al., 2020; Turnbull et al., 2015) and inversion (Lauvaux et al., 2020; Sargent et al., 2018; Wu et al., 2018) studies, but the impact of uncertain biological fluxes has been shown to be large (Lauvaux et al., 2020; Wu et al., 2018), and we have not had direct flux measurements available for evaluating the modeled ecosystem flux priors. Further, a number of studies (Lauvaux et al., 2016; Heimburger et al., 2017) have made the reasonable assumption of neglecting CO₂bio fluxes in the dormant season. This work shows that urban ecosystems in Indianapolis are moderately active even in the cold season. More urban flux measurements are needed to study the range of urban ecosystem CO₂ fluxes.

Conflict of Interest

The authors declare no competing interests.

Data Availability Statement

The Hestia inventory is available online (<https://hestia.rc.nau.edu/>), and other data used in this analysis are available on the INFLUX website (<http://sites.psu.edu/influx/>).

Acknowledgments

The authors thank Bernd J. Haupt (PSU) for data acquisition and quality control. This work was funded by the National Institute of Standards and Technology (Project 70NANB10H245). T. Lauvaux was supported by the French research program Make Our Planet Great Again (Project CIUDAD). K.R. Gurney, J. Liang, and G. Roest received support from the National Aeronautics and Space Administration (Grant NNX14AJ20G) and the National Institute of Standards and Technology (Grant 70NANB16H264N).

277

References

278

Ao, X., Grimmond, C., Chang, Y., Liu, D., Tang, Y., Hu, P., ... Tan, J. (2016). Heat, water and carbon exchanges in the tall megacity of Shanghai: challenges and results. *International Journal of Climatology*, *36*(14), 4608–4624.

279

280

281

Aubinet, M., Vesala, T., & Papale, D. (2012). *Eddy covariance: a practical guide to measurement and data analysis*. Springer Science & Business Media.

282

283

284

Basu, S., Lehman, S. J., Miller, J. B., Andrews, A. E., Sweeney, C., Gurney, K. R., ... Tans, P. P. (2020). Estimating US fossil fuel CO₂ emissions from measurements of ¹⁴C in atmospheric CO₂. *Proceedings of the National Academy of Sciences*, *117*(24), 13300–13307.

285

286

287

Basu, S., Miller, J. B., & Lehman, S. (2016). Separation of biospheric and fossil fuel fluxes of CO₂ by atmospheric inversion of CO₂ and ¹⁴CO₂ measurements: observation system simulations. *Atmospheric Chemistry and Physics*, *16*(9), 5665–5683.

288

289

290

291

Björkegren, A., & Grimmond, C. (2018). Net carbon dioxide emissions from central London. *Urban Climate*, *23*, 131–158.

292

293

294

Boden, T. A., Marland, G., & Andres, R. J. (2009). Global, regional, and national fossil-fuel CO₂ emissions. *Carbon Dioxide Information Analysis Center, Oak Ridge National Laboratory, US Department of Energy, Oak Ridge, Tenn., USA*, *10*.

295

296

297

Bréon, F., Broquet, G., Puygrenier, V., Chevallier, F., Xueref-Remy, I., Ramonet, M., ... others (2015). An attempt at estimating Paris area CO₂ emissions from atmospheric concentration measurements. *Atmospheric Chemistry and Physics*, *15*(4), 1707–1724.

298

299

300

Bulkeley, H. (2013). *Cities and Climate Change*. London: Routledge.

301

302

Burba, G., & Anderson, D. (2010). *A brief practical guide to eddy covariance flux measurements: principles and workflow examples for scientific and industrial applications*. Li-Cor Biosciences.

303

304

Chaouad, R., & Verzeroli, M. (2018). The urbanization of the world: Facts and challenges. *Revue internationale et strategique*(4), 47–65.

305

306

307

Christen, A., Coops, N., Crawford, B., Kellett, R., Liss, K., Olchovski, I., ... Voogt, J. (2011). Validation of modeled carbon-dioxide emissions from an urban neighborhood with direct eddy-covariance measurements. *Atmospheric Environment*, *45*(33), 6057–6069.

308

309

310

Davis, K. J., Deng, A., Lauvaux, T., Miles, N. L., Richardson, S. J., Sarmiento, D. P., ... others (2017). The Indianapolis Flux Experiment (INFLUX): a test-bed for developing urban greenhouse gas emission measurements. *Elem Sci Anth*, *5*.

311

312

313

314

Deng, A., Lauvaux, T., Davis, K. J., Gaudet, B. J., Miles, N., Richardson, S. J., ... others (2017). Toward reduced transport errors in a high resolution urban CO₂ inversion system. *Elem Sci Anth*, *5*.

315

316

317

Edenhofer, O., et al. (2015). *Climate Change 2014: Mitigation of Climate Change* (Vol. 3). Cambridge University Press.

318

319

Foken, T., & Napo, C. J. (2008). *Micrometeorology*. Springer.

320

321

Gately, C., & Hutyra, L. (2017). Large uncertainties in urban-scale carbon emissions. *Journal of Geophysical Research: Atmospheres*, *122*(20), 11–242.

322

323

Grimmond, C., King, T., Cropley, F., Nowak, D., & Souch, C. (2002). Local-scale fluxes of carbon dioxide in urban environments: methodological challenges and results from Chicago. *Environmental Pollution*, *116*, S243–S254.

324

325

Gu, L., Falge, E. M., Boden, T., Baldocchi, D. D., Black, T., Saleska, S. R., ... others (2005). Objective threshold determination for nighttime eddy flux filtering. *Agricultural and Forest Meteorology*, *128*(3-4), 179–197.

326

327

328

Gurney, K. R., Mendoza, D. L., Zhou, Y., Fischer, M. L., Miller, C. C., Geethakumar, S., & de la Rue du Can, S. (2009). High resolution fossil fuel combustion

329

330

- 331 CO₂ emission fluxes for the United States. *Environmental Science & Technol-*
 332 *ogy*, 43(14), 5535–5541.
- 333 Gurney, K. R., Razlivanov, I., Song, Y., Zhou, Y., Benes, B., & Abdul-Massih, M.
 334 (2012). Quantification of fossil fuel CO₂ emissions on the building/street scale
 335 for a large US City. *Environmental Science & Technology*, 46(21), 12194–
 336 12202.
- 337 Hardiman, B. S., Wang, J. A., Hutyra, L. R., Gately, C. K., Getson, J. M., & Friedl,
 338 M. A. (2017). Accounting for urban biogenic fluxes in regional carbon budgets.
 339 *Science of The Total Environment*, 592, 366–372.
- 340 Heimbürger, A. M., Harvey, R. M., Shepson, P. B., Stirm, B. H., Gore, C., Turn-
 341 bull, J., ... others (2017). Assessing the optimized precision of the aircraft
 342 mass balance method for measurement of urban greenhouse gas emission rates
 343 through averaging. *Elem Sci Anth*, 5.
- 344 Hsu, A., Höhne, N., Kuramochi, T., Roelfsema, M., Weinfurter, A., Xie, Y., ... oth-
 345 ers (2019). A research roadmap for quantifying non-state and subnational
 346 climate mitigation action. *Nature Climate Change*, 9(1), 11–17.
- 347 Hutyra, L. R., Duren, R., Gurney, K. R., Grimm, N., Kort, E. A., Larson, E., &
 348 Shrestha, G. (2014). Urbanization and the carbon cycle: Current capabilities
 349 and research outlook from the natural sciences perspective. *Earth's Future*,
 350 2(10), 473–495.
- 351 Ishidoya, S., Sugawara, H., Terao, Y., Kaneyasu, N., Aoki, N., Tsuboi, K., & Kondo,
 352 H. (2020). O₂:CO₂ exchange ratio for net turbulent flux observed in an urban
 353 area of Tokyo, Japan, and its application to an evaluation of anthropogenic
 354 CO₂ emissions. *Atmospheric Chemistry and Physics*, 20(9), 5293–5308.
- 355 Järvi, L., Nordbo, A., Junninen, H., Riikonen, A., Moilanen, J., Nikinmaa, E., &
 356 Vesala, T. (2012). Seasonal and annual variation of carbon dioxide surface
 357 fluxes in Helsinki, Finland, in 2006–2010. *Atmospheric Chemistry and Physics*,
 358 12(18), 8475–8489.
- 359 Kljun, N., Calanca, P., Rotach, M., & Schmid, H. (2004). A simple parameterisation
 360 for flux footprint predictions. *Boundary-Layer Meteorology*, 112(3), 503–523.
- 361 Kljun, N., Calanca, P., Rotach, M., & Schmid, H. P. (2015). A simple two-
 362 dimensional parameterisation for Flux Footprint Prediction (FFP). *Geosci-*
 363 *entific Model Development*, 8(11), 3695–3713.
- 364 Kunik, L., Mallia, D. V., Gurney, K. R., Mendoza, D. L., Oda, T., & Lin, J. C.
 365 (2019). Bayesian inverse estimation of urban CO₂ emissions: results from a
 366 synthetic data simulation over Salt Lake City, UT. *Elem Sci Anth*, 7(1).
- 367 Lauvaux, T., Gurney, K. R., Miles, N. L., Davis, K. J., Richardson, S. J., Deng,
 368 A., ... others (2020). Policy-relevant assessment of urban CO₂ emissions.
 369 *Environmental Science & Technology*, 54(16), 10237–10245.
- 370 Lauvaux, T., Miles, N. L., Deng, A., Richardson, S. J., Cambaliza, M. O., Davis,
 371 K. J., ... others (2016). High-resolution atmospheric inversion of urban CO₂
 372 emissions during the dormant season of the Indianapolis Flux Experiment (IN-
 373 FLUX). *Journal of Geophysical Research: Atmospheres*, 121(10), 5213–5236.
- 374 Leclerc, M. Y., & Foken, T. (2014). *Footprints in Micrometeorology and Ecology*.
 375 Springer.
- 376 Lee, T., & Koski, C. (2014). Mitigating global warming in global cities: comparing
 377 participation and climate change policies of C40 cities. *Journal of Comparative*
 378 *Policy Analysis: Research and Practice*, 16(5), 475–492.
- 379 Lee, X., Massman, W., & Law, B. (2004). *Handbook of Micrometeorology: A guide*
 380 *for surface flux measurement and analysis*. Springer Science & Business Me-
 381 dia.
- 382 Levin, I., & Karstens, U. (2007). Inferring high-resolution fossil fuel CO₂ records at
 383 continental sites from combined ¹⁴CO₂ and CO observations. *Tellus B*, 59(2),
 384 245–250.
- 385 Lietzke, B., Vogt, R., Feigenwinter, C., & Parlow, E. (2015). On the controlling

- 386 factors for the variability of carbon dioxide flux in a heterogeneous urban
 387 environment. *International Journal of Climatology*, *35*(13), 3921–3941.
- 388 McKain, K., Wofsy, S. C., Nehrkorn, T., Eluszkiewicz, J., Ehleringer, J. R., &
 389 Stephens, B. B. (2012). Assessment of ground-based atmospheric observations
 390 for verification of greenhouse gas emissions from an urban region. *Proceedings*
 391 *of the National Academy of Sciences*, *109*(22), 8423–8428.
- 392 Menzer, O., & McFadden, J. P. (2017). Statistical partitioning of a three-year time
 393 series of direct urban net CO₂ flux measurements into biogenic and anthro-
 394 pogenic components. *Atmospheric Environment*, *170*, 319–333.
- 395 Miles, N. L., Richardson, S. J., Lauvaux, T., Davis, K. J., Balashov, N. V., Deng,
 396 A., ... others (2017). Quantification of urban atmospheric boundary layer
 397 greenhouse gas dry mole fraction enhancements in the dormant season: results
 398 from the Indianapolis Flux Experiment (INFLUX). *Elem Sci Anth*, *5*.
- 399 Miller, J. B., Lehman, S. J., Montzka, S. A., Sweeney, C., Miller, B. R., Karion,
 400 A., ... others (2012). Linking emissions of fossil fuel CO₂ and other anthro-
 401 pogenic trace gases using atmospheric ¹⁴CO₂. *Journal of Geophysical Research:*
 402 *Atmospheres*, *117*(D8).
- 403 Miller, J. B., Lehman, S. J., Verhulst, K. R., Miller, C. E., Duren, R. M., Yadav, V.,
 404 ... Sloop, C. D. (2020). Large and seasonally varying biospheric CO₂ fluxes in
 405 the Los Angeles megacity revealed by atmospheric radiocarbon. *Proceedings of*
 406 *the National Academy of Sciences*, *117*(43), 26681–26687.
- 407 Nemitz, E., Hargreaves, K. J., McDonald, A. G., Dorsey, J. R., & Fowler, D. (2002).
 408 Micrometeorological measurements of the urban heat budget and CO₂ emis-
 409 sions on a city scale. *Environmental Science & Technology*, *36*(14), 3139–
 410 3146.
- 411 Oda, T., Bun, R., Kinakh, V., Topylko, P., Halushchak, M., Marland, G., ... oth-
 412 ers (2019). Errors and uncertainties in a gridded carbon dioxide emissions
 413 inventory. *Mitigation and Adaptation Strategies for Global Change*, *24*(6),
 414 1007–1050.
- 415 Olivier, J., & Janssens-Maenhout, G. (2012). CO₂ emissions from fuel combustion.
 416 *IEA CO₂ report*.
- 417 Pataki, D., Alig, R., Fung, A., Golubiewski, N., Kennedy, C., McPherson, E., ...
 418 Romero Lankao, P. (2006). Urban ecosystems and the North American carbon
 419 cycle. *Global Change Biology*, *12*(11), 2092–2102.
- 420 Pataki, D., Xu, T., Luo, Y. Q., & Ehleringer, J. R. (2007). Inferring biogenic and
 421 anthropogenic carbon dioxide sources across an urban to rural gradient. *Oe-*
 422 *ecologia*, *152*(2), 307–322.
- 423 Reinmann, A. B., Smith, I. A., Thompson, J. R., & Hutyra, L. R. (2020). Urban-
 424 ization and fragmentation mediate temperate forest carbon cycle response to
 425 climate. *Environmental Research Letters*, *15*(11), 114036.
- 426 Richardson, S. J., Miles, N. L., Davis, K. J., Lauvaux, T., Martins, D. K., Turnbull,
 427 J. C., ... Cambaliza, M. O. L. (2017). Tower measurement network of in-situ
 428 CO₂, CH₄ and CO in support of the Indianapolis Flux (INFLUX) Experiment.
 429 *Elem Sci Anth*, *5*.
- 430 Sargent, M., Barrera, Y., Nehrkorn, T., Hutyra, L. R., Gately, C. K., Jones, T., ...
 431 others (2018). Anthropogenic and biogenic CO₂ fluxes in the Boston urban
 432 region. *Proceedings of the National Academy of Sciences*, *115*(29), 7491–7496.
- 433 Sarmiento, D. P., Davis, K. J., Deng, A., Lauvaux, T., Brewer, A., & Hardesty, M.
 434 (2017). A comprehensive assessment of land surface-atmosphere interactions in
 435 a WRF/Urban modeling system for Indianapolis, IN. *Elem Sci Anth*, *5*.
- 436 Silva, S. J., Arellano, A. F., & Worden, H. M. (2013). Toward anthropogenic com-
 437 bustion emission constraints from space-based analysis of urban CO₂/CO
 438 sensitivity. *Geophysical Research Letters*, *40*(18), 4971–4976.
- 439 Stauffer, J., Broquet, G., Bréon, F.-M., Puygrenier, V., Chevallier, F., Xueref-Rémy,
 440 I., ... others (2016). The first 1-year-long estimate of the Paris region fossil

- 441 fuel CO₂ emissions based on atmospheric inversion. *Atmospheric Chemistry*
442 *and Physics*, 16(22), 14703–14726.
- 443 Stull, R. B. (2012). *An Introduction to Boundary Layer Meteorology*. Springer Sci-
444 ence & Business Media.
- 445 Sugawara, H., Ishidoya, S., Terao, Y., Takane, Y., Kikegawa, Y., & Nakajima,
446 K. (2021). Anthropogenic CO₂ emissions changes in an urban area of
447 Tokyo, Japan, due to the COVID-19 pandemic: A case study during the
448 state of emergency in April–May 2020. *Geophysical Research Letters*, 48(15),
449 e2021GL092600.
- 450 Turnbull, J., Karion, A., Davis, K. J., Lauvaux, T., Miles, N. L., Richardson, S. J.,
451 ... others (2018). Synthesis of urban CO₂ emission estimates from multi-
452 ple methods from the Indianapolis Flux Project (INFLUX). *Environmental*
453 *Science & Technology*, 53(1), 287–295.
- 454 Turnbull, J., Sweeney, C., Karion, A., Newberger, T., Lehman, S. J., Tans, P. P., ...
455 others (2015). Toward quantification and source sector identification of fossil
456 fuel CO₂ emissions from an urban area: results from the INFLUX experiment.
457 *Journal of Geophysical Research: Atmospheres*, 120(1), 292–312.
- 458 Turnbull, J. C., Miller, J., Lehman, S., Tans, P., Sparks, R., & Southon, J. (2006).
459 Comparison of ¹⁴CO₂, CO, and SF₆ as tracers for recently added fossil fuel
460 CO₂ in the atmosphere and implications for biological CO₂ exchange. *Geo-*
461 *physical Research Letters*, 33(1).
- 462 Turner, A. J., Shusterman, A. A., McDonald, B. C., Teige, V., Harley, R. A., &
463 Cohen, R. C. (2016). Network design for quantifying urban CO₂ emissions:
464 assessing trade-offs between precision and network density. *Atmospheric Chem-*
465 *istry and Physics*, 16(21), 13465–13475.
- 466 Velasco, E., & Roth, M. (2010). Cities as net sources of CO₂: review of atmospheric
467 CO₂ exchange in urban environments measured by eddy covariance technique.
468 *Geography Compass*, 4(9), 1238–1259.
- 469 Vickers, D., & Mahrt, L. (1997). Quality control and flux sampling problems for
470 tower and aircraft data. *Journal of Atmospheric and Oceanic Technology*,
471 14(3), 512–526.
- 472 Vogt, R., Christen, A., Rotach, M., Roth, M., & Satyanarayana, A. (2006). Tempo-
473 ral dynamics of CO₂ fluxes and profiles over a Central European city. *Theoreti-*
474 *cal and Applied Climatology*, 84(1-3), 117–126.
- 475 Wu, D., Lin, J. C., Duarte, H. F., Yadav, V., Parazoo, N. C., Oda, T., & Kort,
476 E. A. (2021). A model for urban biogenic CO₂ fluxes: Solar-Induced Fluores-
477 cence for Modeling Urban biogenic Fluxes (SMUrF v1). *Geoscientific Model*
478 *Development*, 14(6), 3633–3661.
- 479 Wu, K., Lauvaux, T., Davis, K. J., Deng, A., Coto, I. L., Gurney, K. R., & Patara-
480 suk, R. (2018). Joint inverse estimation of fossil fuel and biogenic CO₂ fluxes
481 in an urban environment: An observing system simulation experiment to assess
482 the impact of multiple uncertainties. *Elem Sci Anth*, 6(1).